Deep low-frequency tremors as a proxy for slip monitoring at plate interface

Deep low-frequency tremors as a proxy for slip monitoring at plate interface

Yoshihiro Hiramatsu and Tomoko Watanabe*

Graduate School of Natural Science and Technology, Kanazawa University

Kakuma, Kanazawa, Ishikawa 920-1192, Japan

Kazushige Obara

National Research Institute for Earth Science and Disaster Prevention

3-1, Tennodai, Tsukuba, Ibaraki 305-0006, Japan

Corresponding author: Yoshihiro Hiramatsu

E-mail: yoshizo@hakusan.s.kanazawa-u.ac.jp Phone: +81-76-264-6519

*Now at: ABB Bailey Japan Limited

511 Baraki, Izunokuni-shi, Shizuoka, 410-2193, Japan

E-mail: tomoko_watanabe@bailey.co.jp Phone: +81-55-949-8822

E-mail: obara@bosai.go.jp Phone: +81-29-863-7626

Abstract

We propose a new method to monitor slip at the plate interface using non-volcanic deep-low frequency (DLF) tremors. We assume that a DLF tremor is the superposition of frequently excited intermittent events, meaning that the envelope of the reduced displacement of the DLF tremor provides an apparent moment rate function. We estimate a conversion factor from the apparent moment to the seismic moment with an assumption that a total size of DLF tremors of an episode is proportional to the size of corresponding slow slip event (SSE). The cumulative seismic moment estimated by DLF tremors is consistent with that estimated from geodetic methods and provides appropriate slip and slip rate at the plate interface. This proves our assumptions and demonstrates that DLF tremors are useful tool for real-time monitoring of the slip at the plate interface.

1. Introduction

Subduction of tectonic plates is characterized by stable sliding and unstable sliding at the plate interface. Laboratory experiments and simulation studies reveal that frictional parameters, for example a-b of the rate- and state- friction law [***Dieterich***, 1979], on the plate interface control the slip behavior at the interface. Recent seismological and geodetic observations from dense networks have revealed characteristic phenomena at the transition zone; non-volcanic DLF tremors, very low-frequency earthquakes (VLF) and slow slip events (SSE) [See a review of *Schwartz and Rokosky*, 2007]. *Obara* [2002] first discovered that DLF tremors are distributed parallel to the strike of a subduction zone about 30~40 km in depth in southwest Japan. This location corresponds to the transition from unstable to stable slip on the plate interface, suggesting that DLF tremors are important to understand the seismogenic process of a large earthquake on the interface.

Causes of non-volcanic DLF tremors are considered to be associated with fluid [*Obara*, 2002; *McCausland et al*., 2005; *Miyazawa and Mori*, 2006], hydroseismogenic processes [*Kao et al*., 2006], shearing at the interface [*Rogers and Dragert*, 2003; *Shelly et al*., 2006] and at deformation zone above the interface [*Kao et*

al., 2006]. *Watanabe et al*. [2007] showed that the amplitude-duration distribution of DLF tremors followed not a power law as regular earthquakes but an exponential law. They suggested that a fixed source dimension with variable excess pressure of fluid or variable stress drop at shear slip possibly caused the tremors.

One of the most important features of the tremors is a spatial and temporal correlation with SSE referred to as episodic tremor and slip (ETS). Such a correlation is found in Cascadia [*Rogers and Dragert*, 2003; *Kao et al*., 2006] and in southwest Japan [*Obara et al*., 2004; *Hirose and Obara*, 2005, 2006; *Obara and Hirose*, 2006].

A relationship between the size of SSE and the tremor activity is, however, not clear. *Ide et al*. [2007] reported that the seismic moment of events on the plate interface, such as SSEs, VLFs and LFEs, is proportional to the duration of the events. The total duration of DLF tremors during an SSE has also been shown to be proportional to the seismic moment of the event [*Aguiar et al*., 2006]. On the other hand, the magnitude of the reduced displacement of DLF tremors is not related directly to the size of the associated SSE [*McCausland et al*. ,2005; *Rokosky et al*., 2006]. We, thus, try to quantify the size of the tremors as a function of both the magnitude and the duration

of the tremors in order to relate to the size of SSE.

In this paper, we assume the envelope of the reduced displacement as an apparent moment rate function. We note a long-term average value of the apparent moment to avoid the fluctuation of relationships between the size of SSE and the tremor activity. We estimate slip and slip rate on the plate interface from DLF tremors in the Tokai region, Japan, with the conversion factor from the apparent moment of the DLF tremors to the seismic moment using an associated SSE. The obtained values of the cumulative seismic moment, the slip and the slip rate on the plate interface are consistent with that estimated by geodetic measurements.

2. Data

We analyze waveform data recorded by a nationwide high-sensitivity seismograph network (Hi-net) [*Obara et al*., 2005] over Japanese Islands operated by National Research Institute for Earth Science and Disaster Prevention (NIED). We search the DLF tremors with a good S/N ratio around the time of low-frequency events

whose magnitudes (M_{JMA}) are greater than 0.3 reported by the Japan Meteorological Agency (JMA) because a low-frequency event is usually included in a DLF tremor. In this study, we use DLF tremors whose duration of the reduced displacement, which is 1.5 times greater than noise level, is longer than 30 s. Finally, we analyze 391 DLF tremors that occurred in the Tokai region from November 2002 to January 2006 (Figure 1a). We use the location of the JMA event as the source of a tremor. Some tremors we analyzed here include several JMA events. In this case we define the hypocenter location of the largest event as that of a tremor. A space-time distribution of the DLF tremors shows episodic occurrences of the DLF tremors and high activity in the central part of the analyzed area (Figure 1b). We select five Hi-net stations in the Tokai region, Asahi (ASHH), Asuke (ASUH), Horai (HOUH), Shidara (STRH), Tukude (TDEH) (Figure 1), which provide high S/N waveform data of the DLF tremors [*Watanabe et al.*, 2007] and are located above the high activity area in the central part.

3. Apparent moment estimated from reduced displacement of DLF tremors

We convert the observed tremor amplitudes to reduced displacements to estimate an apparent seismic moment of DLF tremors. The reduced displacement is RMS ground displacement corrected for the geometrical spreading and is in distance×amplitude (m^2) [*Aki and Koyanagi*, 1981]. We apply the band-pass filter of 2~10 Hz and the moving average with the time window of 6 s for root-mean-squared (RMS) ground displacement [*Watanabe et al.*, 2007]. We calculate the reduced displacement using the formula, $D_R = A \cdot r / 2\sqrt{2}$, for body waves [*Aki and Koyanagi*, 1981] where A is the RMS ground displacement and r the distance between a source and a receiver, with an assumption that a DLF tremor is mainly composed of S waves [*Obara*, 2002; *Rogers and Dragert*, 2003].

DLF tremors are considered to be a superposition of frequently excited low-frequency events [e.g. *Shelly et al.*, 2007]. If this is the case, we can regard the reduced displacement of a DLF tremor as a moment rate function of the tremor because a pulse of far-field displacement approximately represents the moment rate function of an earthquake [*Aki and Richards*, 1980]. Based on this approximation we estimate apparent moment as the event size of a DLF tremor from the average of the time

integral of the reduced displacement at the five stations. The apparent moment of a DLF tremor varies with station due to mainly site effect. The variation is, however, almost constant, meaning that introducing a scaling factor for each station can provide approximately the same apparent moment and cumulative one. This shows also that the average value of the apparent moment using these stations is affected little by the location of the sources of DLF tremors in this study.

Some DLF tremors are excited by dynamic stress perturbation, for example a passage of large amplitude surface waves [*Miyazawa and Mori*, 2006]. In this study, we neither identify nor exclude those tremors in the calculation because the size of those tremors could be small enough such that the following discussion is unaffected.

4. Size distribution of DLF tremors using apparent moment

The size distribution of a phenomenon is important to understand the physical process of the phenomena. Figure 2 shows the size distribution of the apparent moment of the DLF tremors whose apparent moment is greater than 3.0×10^{-3} m^2s. We fit two

models to the distribution; one is the exponential model and the other the power law model referred to as the Gutenberg-Richter relationship [*Gutenberg and Richter*, 1954]. The coefficient of determination, R^2, of the exponential model is larger than that of the power law model (Figure 2a, 2b). This significance becomes clearer if we fit the models for data excluding the largest five events that lack continuity of the distribution of the apparent moment (Figure 2c, 2d). Figure 2 clearly shows that the size distribution of the apparent moment obeys the exponential model rather than the power law model. This is consistent with the result of the duration-amplitude distribution of DLF tremors, suggesting that the source process of the DLF tremors differs from that of regular earthquakes [*Watanabe et al.*, 2007]. If we choose 0.01 m^2s as a cut-off, we cannot find any differences in fitting of both models.

5. Slip and slip rate on the plate interface inferred from DLF tremors

Figure 3d shows a temporal variation in the cumulative apparent moment of the DLF tremors from November 2002 to January 2006. The value of the cumulative

apparent moment on January 2006 is 3.77 m^2s.

Hirose and Obara [2006] reported that short-term SSEs and DLF tremors occurred synchronously on December 2004, July 2005 and January 2006 in the Tokai region from the records of tilt-meters operated by NIED. A coverage of the tile-meter stations of the 2005 event is good and the calculations show good consistency with the observations, providing more accurate fault model of the SSE than the others. We, thus, use this event to estimate the conversion factor from apparent moment to seismic moment. In the calculation, we assume that a total apparent moment of an episode is proportional to the size of a SSE on the plate interface.

The seismic moment of the 2005 event was 5.3×10^{17} Nm [*Hirose and Obara*, 2006] and the total apparent moment of the DLF tremors corresponding to the 2005 event is 0.566 m^2s, providing the conversion factor of 9.36×10^{17} N/m/s. Applying this value, we can estimate that the cumulative seismic moment derived by the DLF tremors is 3.53×10^{18} Nm during the whole analyzed period (Figure 3d).

There is another work of SSEs in the Tokai region based on geodetic data. *Kobayashi et al*. [2006] investigated the occurrence of short-term SSEs in the Tokai

region from 1984 to 2005 using the records of volumetric and multi-component strain-meters operated by JMA. From careful analyses of strain changes, they found 14 short-term SSEs, including the 2005 event reported by *Hirose and Obara* [2006], during the period in this study. We find clear positive correlations between the seismic moment of the 14 SSEs and the total apparent moment of the corresponding episode of DLF tremors (correlation coefficient (R) =0.75) (Figure 3a) and between the seismic moment and the total duration of the DLF tremors (R=0.71) (Figure 3b). These mean that the apparent moment is mainly proportional to the duration as shown in the case of slow earthquakes [*Ide et al*., 2007]. A clear correlation between the seismic moment of SSEs and the apparent moment suggests that our approach for the estimation of the seismic moment using DLF tremors is appropriate, and also supports the validity of the assumptions. On the other hand, there are some fluctuations in the relationship, suggesting a spatial-temporal variation in the conversion factor. However, the fluctuations may arise as a result of uncertainties of analyses of SSEs. It is, thus, difficult to mention a spatial-temporal variation in the conversion factor in this study. A weak positive correlation (R=0.42) between the seismic moment of SSEs and the

average magnitude of reduced displacement (Figure 3c) implies that the size of DLF tremors is properly represented not by the duration but by the apparent moment although the difference is very small.

Figure 3d shows the cumulative seismic moment estimated from the results of *Kobayashi et al*. [2006] from November 2002 to August 2005. The value of cumulative seismic moment on August 2005 is 3.6×10^{18} Nm. Considering the uncertainties of the fault models of the SSEs, this value is consistent with that of 3.0×10^{18} Nm estimated from the DLF tremors for the same period. The cumulative seismic moment based on the duration of the DLF tremors using the same procedure is slightly larger than that of the apparent moment (Figure 3d).

A basic concept of this study is that DLF tremors and SSEs are phenomena that relate quantitatively to the slip at the plate interface. The conversion factor is, therefore, a kind of energy partitioning factors of the strain energy release at the plate interface. Recently, for slow earthquakes, *Ide et al*. [2008] reported that moment rate functions estimated by waveform inversion were proportional to squared velocity waveforms in the 2-8 Hz band, observed usually as DLF tremors, as radiated energy

functions, that is, the scaled energy [*Kanamori and Rivera*, 2006] is nearly constant. If this relationship is expanded for the DLF tremors and the SSEs, the conversion factor is possibly interpreted to be proportional to the inverse of the scaled energy, that is, a ratio of seismic moment of SSEs to radiated energy of DLFs.

The distribution of the DLF tremors used in this study covered the whole fault areas of the short-term SSEs of *Kobayashi et al*. [2006]. We confirm that the areas with high activity of the DLF tremors are consistent with the total fault area of *Kobayashi et al*. [2006]. We, therefore, assume that the cumulative seismic moment of DLF tremors relates approximately to the slip on the total fault area of *Kobayashi et al*. [2006]. We estimate the cumulative slip on the plate interface from the formula of $Mo=\mu US$, where Mo is the cumulative seismic moment, U the cumulative slip, μ the rigidity and S the fault area. Substituting 3.53×10^{18} Nm estimated from the DLF tremors into Mo, 7.14×10^{8} m^2 into S and 40 GPa into μ [*Kobayashi et al*., 2006], we obtain the cumulative slip of 12.4 cm, providing the average slip rate of 3.9 cm/year. The conversion rate of the Philippine Sea plate in this region is estimated to be 3~4 cm/year from GPS observation [*Heki and Miyazaki*, 2001]. The estimated slip rate as the

long-term average from the DLF tremors is consistent with that from geodetic approach, suggesting that the locking of the plate is resolved by SSEs below the seismogenic zone on the plate interface.

6. Activity of DLF tremors, short-term SSEs and a Long-term SSE

We compare the temporal variation in the cumulative moment of the DLF tremors to that in the crustal movement caused by a long-term SSE in the Tokai region [*Ozawa et al*., 2002] in Figures 3d and 3e. The long-term SSE started in the late 2000. The slip of the long-term SSE accelerated up to July 2002, decelerated to the late 2002 and accelerated during 2003 to 2004, and terminated after the late 2004 [*Ozawa et al*., 2005; *Suitou and Ozawa*, 2006]. An active period of DLF tremors indicated by a steep gradient of the cumulative moment curve seems to overlap to the accelerated period of the crustal movement caused by the long-term SSE. In other words, the activity of the DLF tremors corresponds to that of the long-term SSE. Applying the value of the fault area mentioned above, we can estimate the slip rate of 4.2 cm/year for the accelerated

period and 3.5 cm/year for the terminated period.

Furthermore, we can recognize that the recurrence interval of DLF tremors varies with the activity of the long-term SSE that is short in the accelerated period and long in the terminated period (Figures 3d and 3e). *Hirose and Obara* [2005] reported that such a variation in the recurrence interval of DLF tremors with short-term SSE due to the interaction between a long-term SSE and short-term SSEs in Bungo-Suido, Japan. The source areas of short-term SSEs are adjacent to that of a long-term SSE. The slip of the long-term SSE may perturb and concentrate the stress in the surrounding region, causing the short-term SSE with periodic recurrence interval to release the stress on the plate interface in a region and resulting DLF tremors. We, therefore, consider that a relative short recurrence interval of DLF tremors in the accelerated period reflects the rapid stress accumulation on the plate interface due to the long-term SSE and vice-versa. It should be, however, mentioned that *Kobayashi et al*. [2006] found no clear relationship between the activity of SSEs and that of the long-term SSE before 2002.

We show the utility of DLF tremors to monitor the slip on the plate interface in this study. There are, however, some points to be improved, such as how to associate

a region where the slip occurs to an episode of DLF tremors. A better estimation of the conversion factor in space and time will allow us to make a better monitoring of slip distribution at the transition zone from unstable slip to stable slip at the plate interface.

Acknowledgements

We are grateful to National Research Institute for Earth Science and Disaster Prevention and the Japan Meteorological Agency and Hisashi Suito for providing us the data. We thank Ikuro Sumita and Tetsuya Hirose for useful discussion. Comments of two anonymous reviewers are valuable. GMT software [*Wessel and Smith*, 1998] was used to draw all figures.

7. References

Aguiar, A. C., T. I. Melbourne, and C. W. Scrivner (2006), Automated tremor analysis from the Cascadia subduction zone, *Eos Trans. AGU*, 87(52), Fall Meet. Suppl.,

Abstract T41A-1536.

Aki, K., and R. Y. Koyanagi (1981), Deep volcanic tremor and magma ascent mechanism under Kilauea, Hawaii, *J. Geophys. Res*., *86*, 7095-7109.

Aki, K., and P. G. Richards (1980), *Quantitative Seismology*, Vol. 1, W.H. Freeman and Company, New York, 557p.

Dieterich, J. H. (1979), Modeling of rock friction 1. Experimental results and constitutive equations, *J. Geophys. Res., 84*, 2161-2168.

Gutenberg, B., and C. F. Richter (1954), Magnitude and energy of earthquakes, *Ann. Geofis*., *9*, 1-15.

Heki, K., and S. Miyazaki (2001), Plate convergence and long-term crustal deformation in central Japan, *Geophys. Res. Lett*., *28(12)*, 2313-2316.

Hirose, H., and K. Obara (2005), Repeating short- and long-term slow slip events with deep tremor activity around the Bungo channel region, southwest Japan, *Earth Planets Space*, *57*, 961-972.

Hirose, H., and K. Obara (2006), Short-term slow slip and correlated tremor episodes in the Tokai region, central Japan, *Geophys. Res. Lett.*, *33*, L17311, doi: 10. 1029/2006GL026579.

Ide, S., G. C. Beroza, D. R. Shelly, and T. Uchida (2007), A scaling law for slow earthquakes, *Nature*, *447*, doi:10.1038/nature05780.

Ide, S., K. Imanishi, Y. Yoshida, G. C. Beroza, and D. R. Shelly (2008), Bridging the gap between seismically and geodetically detected slow earthquake, *Geophys. Res. Lett.*, *35*, L10305, doi:10.1029/2008GL034014.

Kanamori, H., and L. Rivera (2006), Energy partitioning during an earthquake, AGU Geophysical Monograph Series, 170, 3-13.

Kao, H., S. Shan, H. Dragert, G. Rogers, J. F. Cassidy, K. Wang, T. James, and K. Ramachandran (2006), Spatial-temporal patterns of seismic tremors in northern Cascadia, *J. Geophys. Res., 111*, B03309, doi:10.1029/2005JB003727.

Kobayashi, A., T., Yamamoto, K., Nakamura, and K., Kimura (2006), Short-term slow slip events detected by the strainmeters in Tokai region in the period from 1984 to 2005, *Zisin 2*, *59*, 19-27 (in Japanese with English abstract).

McCausland, W., S. Malone, and D. Johnson (2005), Temporal and spatial occurrence of deep non-volcanic tremor: from Washington to northern California, *Geophys. Res. Lett.*, 32, L24311, doi:10.1029/2005GL024349.

Miyazawa M., and J. Mori (2006), Evidence suggesting fluid flow beneath Japan due to

periodic seismic triggering from the 2004 Sumatra-Andaman earthquake, Geophys. Res. Lett., 33, L05303, doi:10.1029/2005GL025087.

Obara, K. (2002), Nonvolcanic deep tremor associated with subduction in southwest Japan, *Science*, *296*, 1679-1681.

Obara,K., and H. Hirose (2006), Non-volcanic deep low-frequency tremors accompanying slow slips in the southwest Japan subduction zone, *Tectonophys*., *417*, 33-51.

Obara, K., H. Hirose, F. Yamamizu, and K. Kasahara (2004), Episodic slow slip events accompanied by non-volcanic tremors in southwest Japan subduction zone, *Geophys. Res. Lett., 31*, L23602, doi:10. 1029/2004GL020848.

Obara, K., Kasahara, K., Hori, S., and Okada, Y. (2005), A densely distributed high-sensitivity seismograph network in Japan: Hi-net by National Research Institute

for Earth Science and Disaster Prevention, *Review of Scientific Instruments*, *76*, 021301-doi:10.1063/1.1854197.

Ozawa, S., M. Murakami, M. Kaidzu, T. Tada, T. Sagiya, Y. Hatanaka, H. Yarai,, and T. Nishimura (2002), Detection and monitoring of ongoing aseismic slip in the Tokai region, central Japan, *Science*, *298*, 1009-1012.

Ozawa, S., M. Murakami, M. Kaidzu, and Y. Hatanaka (2005), Transient crustal deformation in Tokai region, central Japan, until May 2004, *Earth Planets Space*, *57*, 909-915.

Rogers, G., and H. Dragert (2003), Episodic tremor and slip on the Cascadia subduction zone: The chatter of silent slip, *Science*, *300*, 1942-1943.

Rokosky, J. M., S. Y. Schwartz, and K. Obara (2006), Characteristics of subduction zone tremor in SW Japan, *Eos Trans. AGU*, 87(52), Fall Meet. Suppl., Abstract V41A-1699.

Schwartz S.Y., and J.M. Rokosky (2007), Slow slip events and seismic tremor at circum-Pacific subduction zones, *Rev. Geophys*., *45*, RG3004, doi:10.1029/2006RG000208.

Shelly, D.R., G.C. Beroza, S. Ide, and S. Nakamura (2006), Low-frequency earthquakes in Shikoku, Japan and their relationship to episodic tremor and slip, *Nature*, *442*, 188-191.

Shelly, D.R., G.C. Beroza, S. Ide (2007), Non-volcanic tremor and low frequency earthquake swarms, *Nature, 446*, 305-307.

Suito, H, and S. Ozawa (2006), Possibility of migration of Tokai slip, Fall Meeting of

Seismological Society of Japan, P021 (in Japanese).

Watanabe, T., Y. Hiramatsu, and K. Obara (2007), Scaling relationship between the duration and the amplitude of non-volcanic deep low-frequency tremors, *Geophys. Res. Lett.*, *34*, L07305, doi:10.1029/2007GL029391.

Wessel, P., and W. H. F. Smith (1998), New improved version of the Generic Mapping Tools released, *EOS Trans. AGU*, 79, 579.

Figure captions

Figure 1. (a) The distribution of the epicenters of DLF tremors (gray circles) and the Hi-net stations (squares) used in this study. Open circles are tremors and dots are regular earthquakes (M_{JMA}≥2.0) shallower than 60km during 2001-2005 reported by JMA. A triangle shows the GPS station whose E-W displacement is shown in Figure 3. Solid rectangles show the surface projection of the faults estimated by *Kobayashi et al.* [2006].

Line A-A' denotes a section of the time-space distribution of the DLF tremors in (b). (b) A time-space distribution, projected on the line A-A' in (a), of the DLF tremors analyzed in this study.

Figure 2. The size distribution of the apparent moment of the DLF tremors: (a) the exponential model and (b) the power law model for all data larger than 3.0×10^{-3} m^2s, and (c) the exponential model and (d) the power law model excluding the largest five events. Black straight lines show the best fit to the model. Gray ones show the best fit with a cut-off of 0.01 m^2s.

Figure 3. Plots of seismic moment of 14 SSEs reported by *Kobayashi et al.* [2006] versus (a) the apparent moment, (b) the duration, and (c) the average magnitude of the reduced displacement of corresponding episodes of DLF tremors. (d) Temporal variation in cumulative apparent moment (left axis), and cumulative seismic moment (right axis) estimated from the apparent moment (black line), that estimated from the duration (dashed line) and that of SSE reported by *Kobayashi et al.* [2006] (gray line).

(e) Time series data of east-west (E-W) displacement, from which the steady state crustal deformation and annual changes are removed, at the Hamakita GPS station denoted by the triangle in Figure 1.

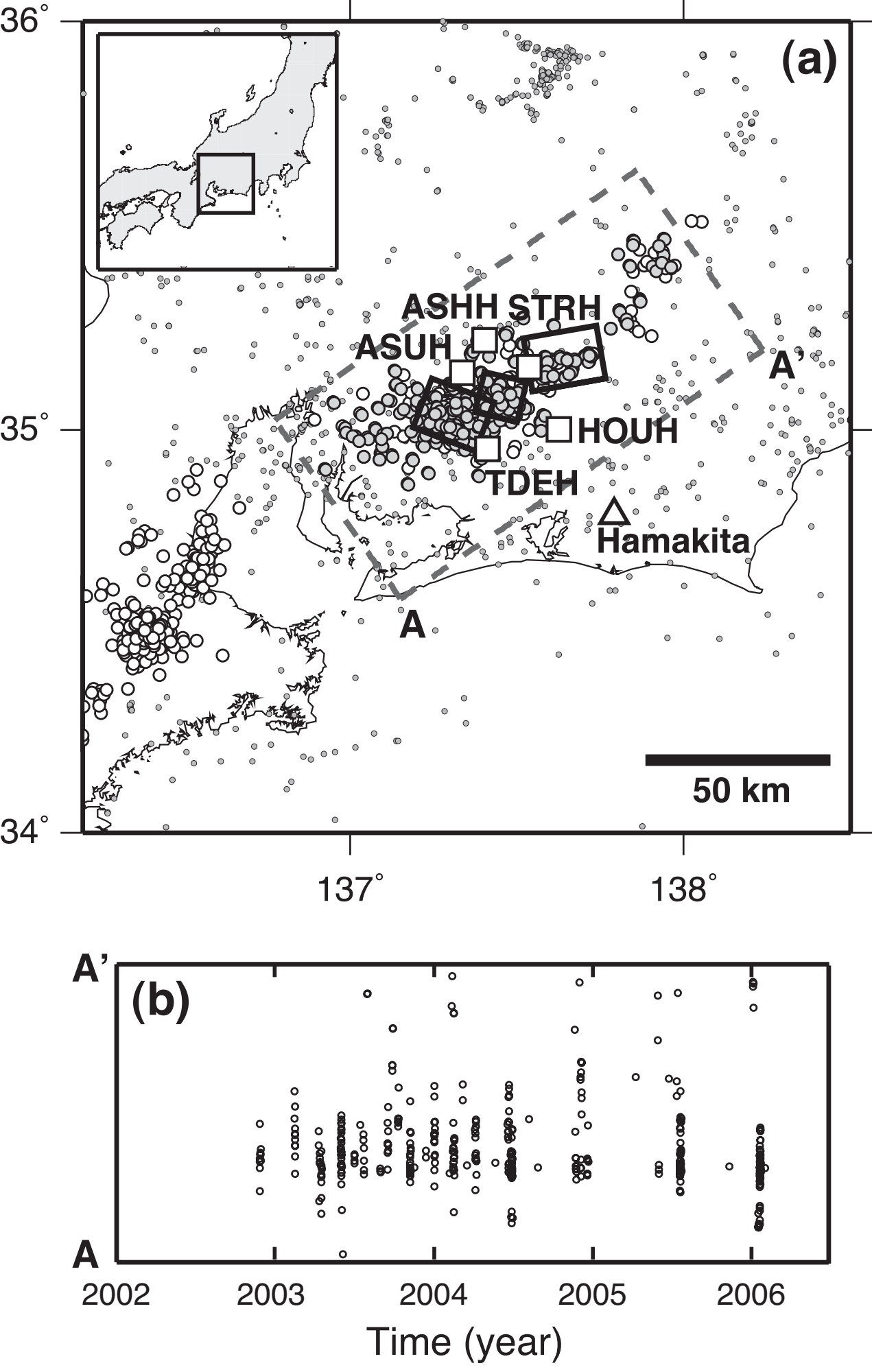
(a)
36°
35°
34°
137°
138°
ASHH
STRH
ASUH
HOUH
TDEH
Hamakita
A
A'
50 km
(b)
A'
A
2002
2003
2004
2005
2006
Time (year)

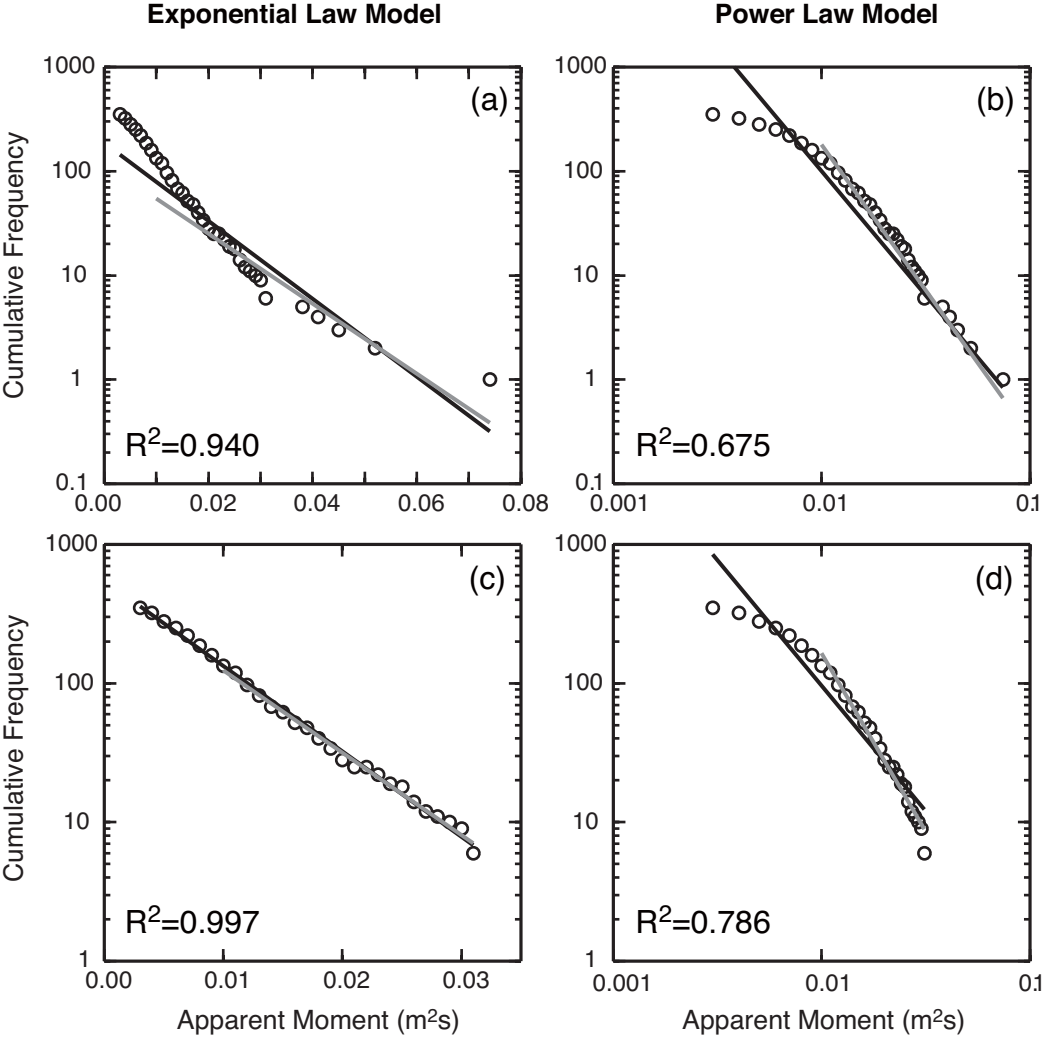
Exponential Law Model
Power Law Model
(a)
(b)
(c)
(d)
Cumulative Frequency
Cumulative Frequency
R2=0.940
R2=0.675
R2=0.997
R2=0.786
1000
100
10
1
0.1
0.00
0.02
0.04
0.06
0.08
0.001
0.01
0.1
0.00
0.01
0.02
0.03
Apparent Moment (m2s)
Apparent Moment (m2s)

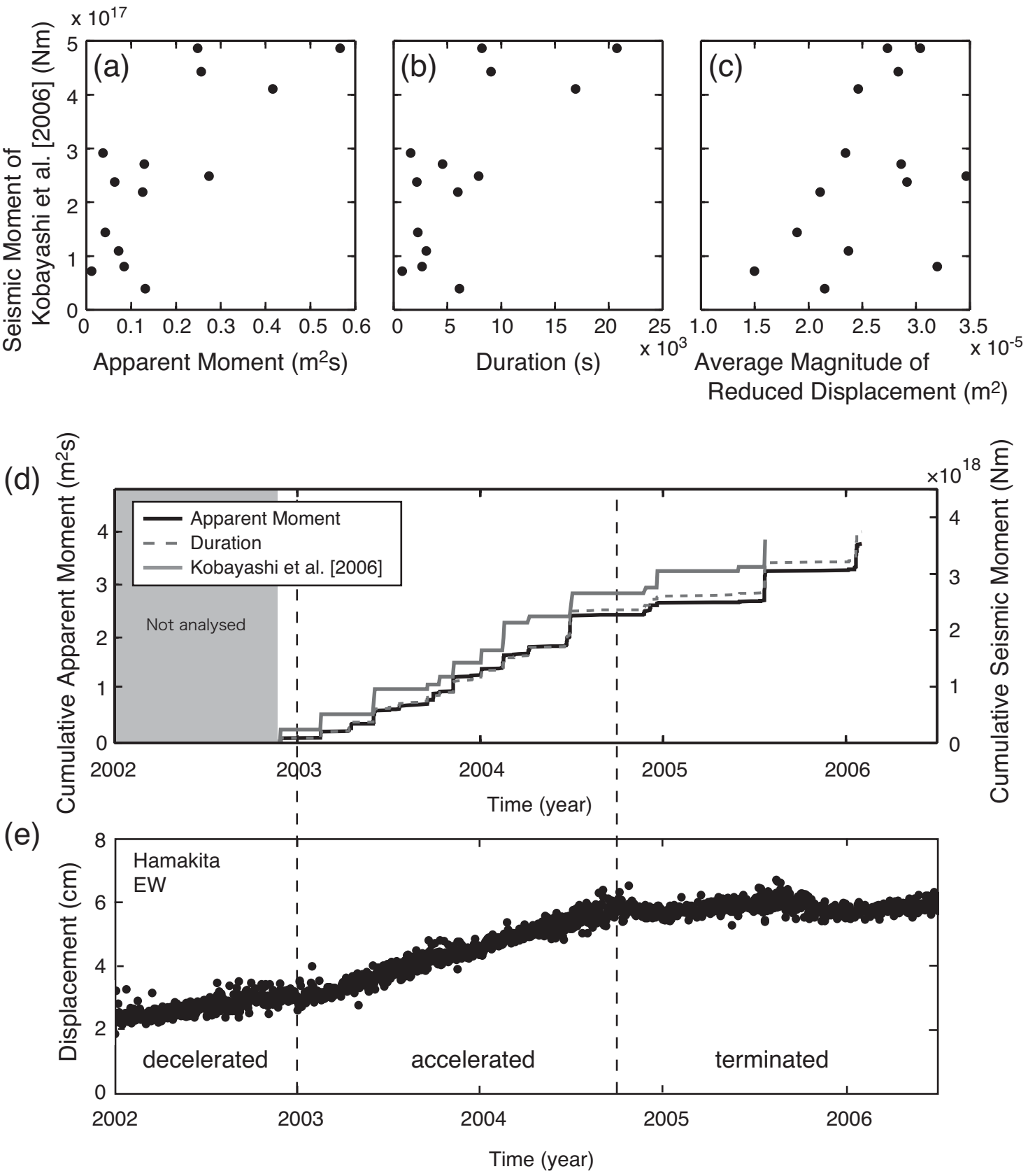
(a)
(b)
(c)
x 10^17
Seismic Moment of Kobayashi et al. [2006] (Nm)
Apparent Moment (m^2s)
Duration (s)
x 10^3
Average Magnitude of Reduced Displacement (m^2)
x 10^-5
(d)
Cumulative Apparent Moment (m^2s)
Cumulative Seismic Moment (Nm)
x10^18
Apparent Moment
Duration
Kobayashi et al. [2006]
Not analysed
Time (year)
(e)
Hamakita
EW
Displacement (cm)
decelerated
accelerated
terminated
Time (year)